GEOPHYSICAL RESEARCH LETTERS, VOL. 39, L19608, doi:10.1029/2012GL053187, 2012

Ocean circulation beneath Larsen C Ice Shelf, Antarctica from *in situ* observations

Keith W. Nicholls,[1] Keith Makinson,[1] and Emily J. Venables[1]

Received 18 July 2012; revised 30 August 2012; accepted 9 September 2012; published 11 October 2012.

[1] Hot-water drilled access holes were used to obtain oceanographic data from beneath two sites on Larsen C Ice Shelf, one in the north and one in the south. At both sites the entire water column was colder than the surface freezing point, and the temperature-salinity characteristics are consistent with a High Salinity Shelf Water source of maximum salinity 34.65 psu. At the southern site the 0.08°C thermal driving at the ice base and the 0.2-m s^{-1} rms water speed resulted in a melt rate of 1.3 ± 0.2 m a^{-1}, as measured over an eight-day period. When combined with the available ship-based data, the evidence suggests that the sub-ice cavity is flushed only by water at the surface freezing point. This implies that the reported decrease in surface elevation of Larsen C Ice Shelf is unlikely to be a result of thinning due to an increasing rate of basal melting. **Citation:** Nicholls, K. W., K. Makinson, and E. J. Venables (2012), Ocean circulation beneath Larsen C Ice Shelf, Antarctica from *in situ* observations, *Geophys. Res. Lett.*, *39*, L19608, doi:10.1029/2012GL053187.

1. Background

[2] The rapid atmospheric warming of the Antarctic Peninsula has led to the sequential north to south break up of several east coast ice shelves: Prince Gustav Ice Shelf (1995), Larsen A Ice Shelf (1995) and most recently, the majority of Larsen B Ice Shelf (2002). *Shepherd et al.* [2003] describe a reduction in surface elevation of the northern Larsen C Ice Shelf between 1992 and 2001, and conclude that this is evidence for an ice-shelf thinning, driven largely by increased ocean melting. They include the caveat that part of the observed surface lowering would have been a result of firn densification due to increased summer air temperatures. *Holland et al.* [2011] present a map of air column thickness for the ice shelf, which shows a strong positive gradient from northwest to southeast, and from which they deduce stronger summer surface melting in the north. They suggest that increasing summer warming, leading to increasing surface melting in the northwest, might account for all the reported surface lowering. *Pritchard et al.* [2012] use ICESat altimetry data to show that the surface lowering continued between 2003 and 2008, and use modeling of the snow surface to support the idea that the lowering is due entirely to surface processes.

[3] For increased basal melting to play a role in the surface lowering, either the currents or water temperatures beneath the ice shelf would need to be increasing. As the only significant drivers of sub-ice shelf currents are thermohaline and tidal, changing currents would require a changing salinity field over the continental shelf.

[4] Adverse sea ice conditions in the northwest Weddell Sea have left the oceanographic conditions over the open Larsen C continental shelf particularly poorly sampled. The most comprehensive dataset was acquired during cruise ANT X/7 of the research ship *Polarstern*, when a conductivity-temperature-depth (CTD) section toward the ice front (Figure 1) and an XBT (eXpendable BathyThermograph) section along the southern two thirds of the ice front were obtained in January 1993 [*Bathmann et al.*, 1994]. Those data showed the continental shelf to be flooded with relatively warm Modified Warm Deep Water (MWDW). However, *Nicholls et al.* [2004] describe a small number of CTD profiles obtained from the northern end of the ice front in March 2002 (Figure 1), and used the properties of the waters flowing out from beneath the ice shelf to show that there was no evidence for flow into the cavity of waters above the surface freezing point. A further contribution to the limited available dataset was made during December 2004 and January 2005 when a helicopter was used to deploy a CTD profiler as part of ISPOL, an ice-drift experiment based on R.V. *Polarstern* [*Hellmer et al.*, 2008]. Although the experiment focused on the Larsen continental shelf break, some of the stations extended westward onto the mid-shelf (Figure 1).

[5] If the *Nicholls et al.* [2004] conclusion that the source waters for the sub-ice shelf circulation are at the surface freezing point is both correct and applicable to the entire ice shelf rather than only its northern part, then this would imply that the conditions beneath the ice shelf cannot be warming, and therefore that the only way the basal melt rate of the ice shelf can be increasing significantly is if the flushing of the cavity is also increasing. A test of the conclusion would require an array of year-round moorings along the ice front to sample the water masses crossing the ice front. As local sea-ice conditions would not routinely allow such an array to be deployed or serviced, a different strategy is required.

[6] A project to study the turbulent boundary layer at the base of ice shelves offered an alternative approach. In December 2011 access holes were drilled through Larsen C Ice Shelf at two sites, one in the south and one in the north (Figure 1). This paper reports on observations of temperature and salinity made beneath both sites, allowing a new assessment of the characteristics of the

[1]British Antarctic Survey, Natural Environment Research Council, Cambridge, UK.

Corresponding author: K. W. Nicholls, British Antarctic Survey, Natural Environment Research Council, High Cross, Madingley Road, Cambridge CB3 0ET, UK. (kwni@bas.ac.uk)

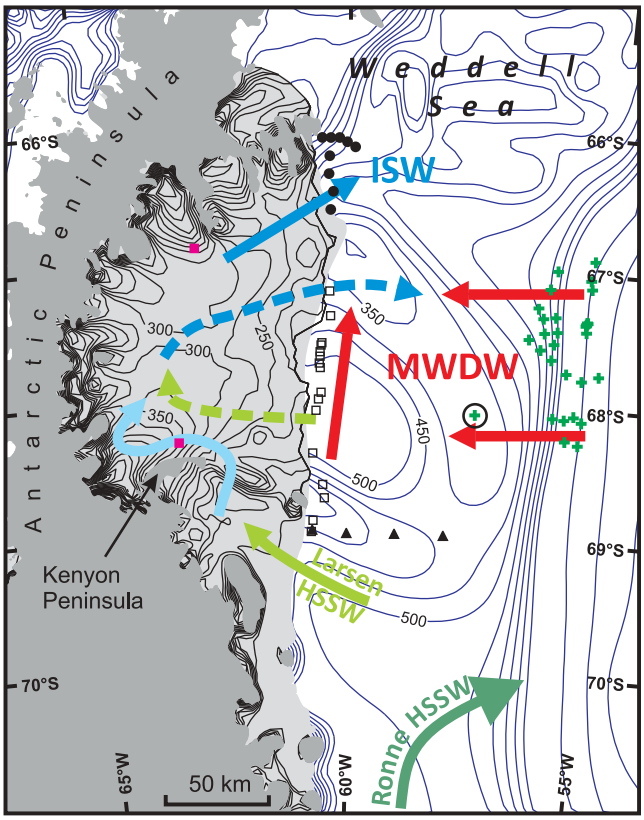

Figure 1. Map showing Larsen C Ice Shelf on the east coast of the Antarctic Peninsula. Contours over the ice shelf (light grey) are of ice thickness; over the ocean (white) they are of water depth (both from *Lythe and Vaughan* [2001]). Red squares indicate the drill sites (Dec 2011); triangles indicate CTD locations from Jan 1993, circles are CTD locations from Mar 2002, squares are XBT stations from Jan 1993 and green crosses are CTD stations from Dec–Jan 2004–05.

source waters supplying the sub-ice shelf cavity. We also report on water currents measured at the southern site.

2. Field Sites and Observations

[7] CTD profiles of the underlying water column were obtained from both drill sites, with thermistor cables being deployed to monitor the temperature in the water column. At the southern site microstructure profiles from the boundary layer were also obtained, and a pair of combined temperature sensors and 3-D current meters were deployed 2.5 and 11.5 m from the ice base, together with an upward-looking sonar (ULS) to monitor basal melting. The data sets to be discussed in this paper are those provided by the current meters, the co-located temperature sensors and the CTD profiles. The time series of current meter data run from when the instruments were deployed to when the site was vacated, giving an eight-day time series; the instruments remain active to provide a long-term record of conditions and melt rates. The ULS was the last instrument to be deployed and a time series is not yet available.

[8] The CTD profiler was a FastCat SBE49, mounted in a stainless steel frame with a Power and Data Interface Module (PDIM) to allow communications with the SBE36 Deck unit. Two holes were drilled at the southern site, allowing two sets of CTD profiles to be obtained, separated by four days. Only one hole was drilled at the northern site. Estimated accuracies of temperature and salinity are 0.004°C and 0.005 psu.

[9] The current meters were Nobska MAVS (Modular Acoustic Velocity Sensor) differential acoustic travel-time instruments, and the temperature sensors were Rockland Scientific International "MicroSquid" systems, based around the FP07 high speed thermistor. The current meter and temperature sensors were programmed to record at 5 Hz for 15 minutes every two hours. Here we discuss only the averages of those 15-minute recording periods.

[10] A direct measurement of the sea floor depth was obtained at each site, allowing point tests of the recently published, gravimetric-based bathymetry for the ice shelf [*Cochran and Bell*, 2012]. The depth at the southern site (S 68° 18.0′, W 063° 21.8′) was 492.8 m, compared with the gravimetric estimate of 500 m. Values for the northern site (S 66° 52.0′, W 062° 54.0′) compare similarly well, with a measured value of 550.5 m, and 540 m from gravimetry. The water column thickness at the southern and northern sites was 192 m and 233 m respectively.

[11] By combining measurements of the depth to the water level within the borehole, the total ice thickness and the density profile of the borehole water as determined from the CTD profiler, we were able to calculate the mean ice shelf density, and therefore the air content of the ice column as a test of the *Holland et al.* [2011] air content map. The southern and northern sites yielded values of 17.6 ± 0.5 m and 7.2 ± 0.5 m, compared with the *Holland et al.* [2011] estimates of 15.3 ± 1.8 and 7.0 ± 1.8 m.

3. Boundary Layer Currents and Temperature

[12] Eight days of data from the two current meters moored in the boundary layer beneath the ice base at the southern site are shown in Figure 2a. The most obvious feature is the dominance of a strong tidal signal: the long-term mean flow is entirely obscured by what appears to be a mixed (diurnal and semidiurnal) tidal variability. As expected, the current meter nearest the ice base is registering a rather weaker signal, and most of the energy at both current meters is in the zonal direction, parallel to the north coast of Kenyon Peninsula, lying east–west some 12 km to the south (Figure 1).

[13] For such a short record, a harmonic tidal analysis is inappropriate. We use the response method [*Munk and Cartwright*, 1966] to determine the tidal ellipses for the seven strongest constituents, three from the diurnal band, and four from the semi-diurnal band (Figure 2b and Table 1). Particularly noticeable is the way in which the ellipses for the diurnal constituents are aligned parallel to the nearby coast, while the semidiurnal ellipses are rotated clockwise. The rotation can be explained by noting that the boundary layer depth differs for different frequencies, and that the ellipse orientation changes as the frictional interface is approached [*Book et al.*, 2009].

[14] Various filters were used to recover the underlying current speed and direction. The most successful approach was singular spectrum analysis [*Vautard et al.*, 1992], which was used to separate the signal into statistically independent components, allowing the selection of those components that constituted the underlying current. Progressive vector

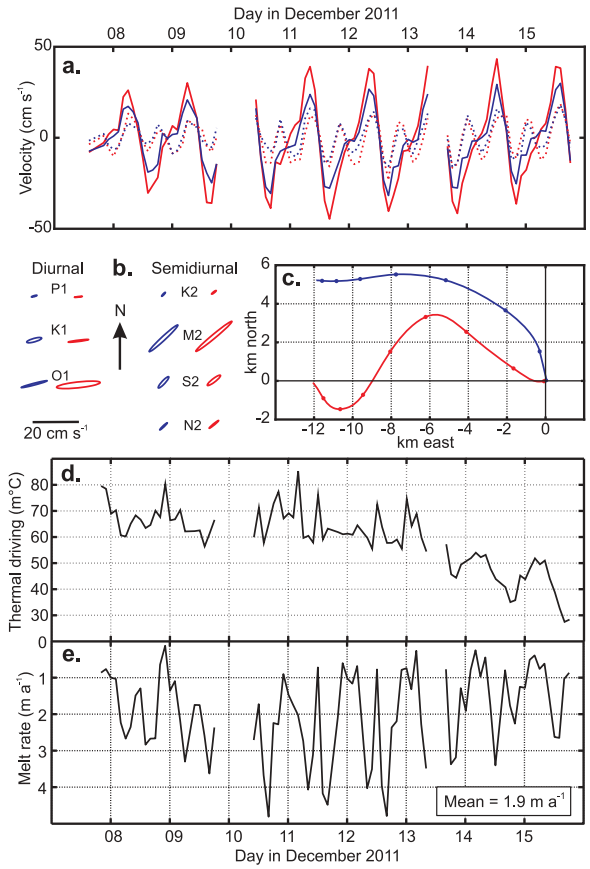

Figure 2. Results from instruments moored 2.5 m and 11.5 m below the ice base at the southern site. (a) Meridional (broken lines) and zonal (solid lines) velocity components from upper (blue) and lower (red) current meters. (b) Current ellipses for selected tidal constituents from upper (blue) and lower (red) current meters. (c) Progressive vector diagrams from filtered current meter records from upper (blue) and lower (red) current meters. (d) Difference between temperature at the upper current meter and the *in situ* freezing point at the ice-base pressure. (e) Melt rate calculated using *Jenkins et al.* [2010] formulation.

diagrams for the two current meters were constructed from the filtered data (Figure 2c), showing a weak westward flow of just under 2 cm s^{-1}. Although the record is only eight days in length and contains a sizable gap, the westward flow for the period of observation was a robust feature of all the filtering methods used.

[15] The two sessions of CTD profiling at the southern site yielded two distinct profiles. In Figure 3a we show the average of 4 profiles, representing the conditions from the first session, and the average of 2 profiles obtained in the second session. At the northern site the shape of the profiles varied noticeably during the single session of profiling, and the averages of two distinct shapes (17 profiles for the first and 6 profiles for the second) are shown in the figure. We speculate that the different profile configurations result from tidally-forced cross-flow motion of horizontal property gradients past the sites.

[16] The two most striking features of the temperature and salinity profiles are the uniformity of properties and the low temperatures: the total range of salinity and temperature at each site is less than 0.05 psu and 0.2°C, and the warmest water observed had a potential temperature of −1.96°C, some 60 m°C below the surface freezing point. Water with a potential temperature below the surface freezing point is defined as Ice Shelf Water (ISW), as it is assumed that it has interacted with an ice-shelf base. At the southern site the potential temperature and salinity deeper than 400 dbar are highly uniform, and a less well-mixed layer occupies the upper 20–30 m of the water column. In the north there are shallow mixed layers (a few tens of meters) at the top and bottom of the water column, with a weak pycnocline between.

[17] Also shown in Figure 3a is the upper 40 m of the *in situ* freezing point profile, adjusted to potential temperature to be comparable with the other profiles shown. At both sites the temperature of the water in the mixed layer adjacent to the ice base is higher than the *in situ* freezing point, indicating a substantial source of heat for melting, particularly in the south. Figure 2d shows the 8-day time series of temperatures measured at the upper current meter at the southern site. The melt rate series shown in Figure 2e was derived by combining the thermal driving found from that time series with the measured currents using the formulation recommended by *Jenkins et al.* [2010]. This yields a mean melt rate for that 8-day period of 1.9 m a^{-1}, although the value is sensitive to the choices of parameters in the formulation used. For the same period, a phase-sensitive radar deployed at the southern site indicated a basal melt rate of around 1.3 ± 0.2 m a^{-1}. The radar measurement gave the thinning rate; to deduce the melt rate the contribution to thinning from the vertical strain rate of the ice has to be accounted for, the estimate of which (from the ice velocity dataset of *Rignot et al.* [2011]) dominated the uncertainty in the measurement.

4. Discussion

[18] The properties of the water masses beneath the ice shelf are most easily discussed by displaying them on a potential temperature-salinity (θ-S) plot. Figure 3b shows the mean data for the two drill sites, together with data obtained from ship-based CTD stations occupied at the southern end of the ice front in early January 1993 [*Bathmann et al.*, 1994], ISPOL helicopter CTD stations from December 2004 to January 2005 [*Absy et al.*, 2008], and some stations at the northern end of the ice front occupied in early March 2002 [*Nicholls et al.*, 2004]. An XBT section along the southern two-thirds of the ice front, also obtained in January 1993 [*Bathmann et al.*, 1994], indicated relatively warm water, with temperatures above −1.6°C to the 500-m maximum depth of the XBTs. The locations of all the ship-based stations are shown in Figure 1.

Table 1. Tidal Constituents From Lower Current Meter (Southern Site)

Species	Semi Maj (cm s^{-1})	Phase (°)	Eccen.	Incl (°)
P1	3.4	111	0.076	7
K1	8.9	119	0.064	7
O1	19.0	61	0.133	6
K2	2.5	172	−0.197	38
M2	20.3	277	−0.084	40
S2	7.1	165	−0.215	37
N2	5.3	230	−0.104	39

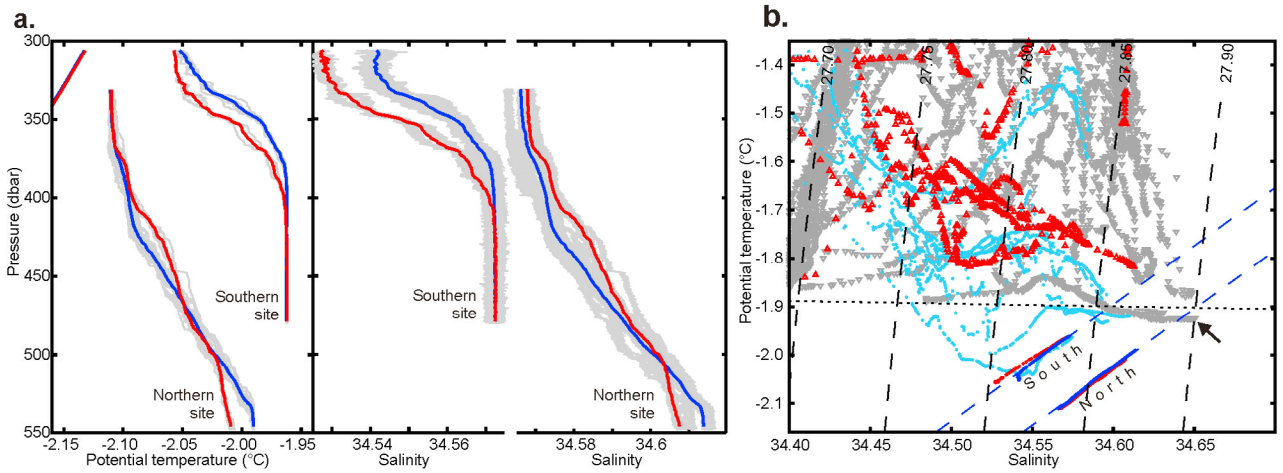

Figure 3. Results from borehole Dec 2011 CTD data. (a) Vertical profiles of θ and S. Blue and red curves are means of two different configurations found at each site, the short near straight lines are the 'potential' freezing point profiles. The grey lines are the original data. (b) θ-S plots for the borehole data (blue and red dots), the 1993 *Polarstern* data (red triangles) [*Bathmann et al.*, 1994], and the 2002 data (cyan circles) [*Nicholls et al.*, 2004]. Dec–Jan 2004–5 data from ISPOL helicopter CTD stations are inverted grey triangles [*Absy et al.*, 2008], the arrowed data corresponding to the circled station in Figure 1. The near horizontal broken line is the surface freezing point, and the two straight, broken lines passing through the borehole data are melt water mixing lines (gradient of 2.42 °C psu^{-1}: see main text). Isopycnals are referenced to surface pressure.

[19] Ignoring the loss of heat into the ice shelf, seawater freezing to form ice at the ice base or seawater melting ice at the ice base will cause its θ-S signature to migrate along a straight line with a gradient of around 2.4°C psu^{-1} [*Gade*, 1979]. In the case of a melting base, when the heat loss into the ice can be significant, the gradient will be slightly higher, perhaps 2.5 or 2.6°C psu^{-1} depending on the basal melt rate and core temperature of the ice shelf. The gradients of the θ-S lines shown in Figure 3b are between 2.55 and 2.57°C psu^{-1}, except for the subset with red markers for the southern site, which had a gradient of 2.32°C psu^{-1}. A lower bound on the source water salinity can be found by noting the intersection between the relevant melt water mixing line and the surface freezing line (Figure 3b). The melt water mixing lines plotted in Figure 3b demonstrate that the waters sampled at both sites are consistent with a source water mass of salinity greater than 34.60 psu. An upper limit of 34.65 is determined by noting that the source water mass for the northern site must lie on its melt water mixing line, which intersects the surface freezing line at 34.65. The only way the source water can have a salinity higher than 34.65 is for it to be above the surface freezing point, which means that it would have consisted of MWDW; we can discount this possibility, however, as the salinity of MWDW is less than 34.60 and there is no mechanism available to raise its salinity at temperatures above the surface freezing point. An upper bound of 34.65 for the salinity of source waters flowing into the Larsen C sub-ice cavity is slightly higher than the value suggested by *Nicholls et al.* [2004].

[20] As found by *Nicholls et al.* [2004], therefore, there is no evidence for waters warmer than the surface freezing point entering the Larsen C cavity, despite the fact that both cruises to the area show that the summertime continental shelf is flooded with MWDW. The potential vorticity step at the ice front presumably acts as a sufficient barrier to flow [e.g., *Grosfeld et al.*, 1997].

[21] The flow at the southern drill site appears to be from east to west, yet the deep water has clearly interacted with an ice base of at least 80-m draft to account for the 60 m°C depression below the surface freezing point. We propose that the High Salinity Shelf Water (HSSW) source for this water mass crossed the ice front southeast of Kenyon Peninsula, interacting with the thin ice shelf that is found there before rounding the peninsula and entering the main Larsen C cavity (Figure 1).

[22] At the northern site the source water salinity (34.65 psu) is significantly higher than found for the southern site. There is more than one possible explanation. If there is an overall south to north circulation exploiting the areas of high water column thickness near the grounding line that are inferred from gravimetry by *Cochran and Bell* [2012], then, assuming a water speed of a few centimeters per second, the time lag between the two sites would be of the order of a few months. Measurements were made at the southern site in early December, and at the northern site about two weeks later, so the salinity of the source waters for the northern site would be likely to be that of shelf waters nearer the height of the freezing season when higher salinities are likely as more sea ice is being produced. The weakness in such a scheme is that the higher densities in the north would be expected to drive a southward flow. An alternative hypothesis is that the water column at the northern site was part of a recirculation driven by a local ice pump, that is, melting in an area of deep ice followed by refreezing at an area of shallow ice base, resulting in salinification and recirculation back to the deeper ice melting area. The net result is a temperature reduction due to repeated episodes of conductive heat loss to the ice shelf. Our favored explanation, however, is that the southern and northern parts of the ice shelf cavity are ventilated from sources crossing beneath the ice front at different locations, as outlined below.

[23] The evidence presented in this paper suggests that the waters entering the Larsen C sub-ice shelf cavity that interact with the ice base are at the surface freezing point, with a salinity of between 34.60 psu and 34.65 psu. This is too fresh to be HSSW produced over the Ronne continental shelf to the south, which has a salinity of greater than 34.7 psu [e.g., *Foldvik et al.*, 1985]. So any HSSW flowing along the continental shelf from the south must drain to the deep Weddell Sea before reaching Larsen C Ice Shelf [e.g., *Gordon*, 1998]. Based on the available observations, we propose the following circulation, illustrated in Figure 1. MWDW crosses the local shelf break and is converted by wintertime sea-ice production into HSSW with a maximum salinity of around 34.65 psu. The HSSW flows beneath the ice front southeast of Kenyon Peninsula where it is chilled by interaction with the relatively shallow ice base before entering the main Larsen C cavity. This is the water mass that travels to the deep grounding lines in the south of the ice shelf and supplies heat for melting, spawning the ISW plumes modeled by *Holland et al.* [2009].

[24] We speculate that an inflow of HSSW into the cavity in the vicinity of the depression at around 68° 20′S is important in the winter (broken line in Figure 1). This is our proposed source for the waters observed at the northern site, which also provides an explanation for the ISW observed by *Absy et al.* [2008] at the ISPOL CTD station circled in Figure 1, and arrowed in Figure 3b. During the summer, however, that part of the ice front is flooded with MWDW [*Bathmann et al.*, 1994], and the evidence presented here suggests that if the MWDW does enter the cavity, it does not interact with the Larsen C Ice Shelf. The ISPOL data suggest that the upper limit for the salinity of waters interacting with the ice-shelf base should be raised to 34.66 psu.

[25] If the temperature of the water interacting with Larsen C Ice Shelf is indeed fixed at the surface freezing point, regulated by sea-ice formation, the only way the basal melt rates can be increasing is if the flux of water through the cavity is increasing. For this to be the case, higher HSSW production rates would be required, necessitating an increasing local ice production. There is little evidence to indicate any significant increasing trend in ice production over the Larsen shelf; indeed, *Hellmer et al.* [2011] have suggested that the waters to the north are freshening, hinting at a reducing local ice production rate for the area.

5. Summary and Conclusions

[26] We have presented CTD profiles from beneath Larsen C Ice Shelf from one site in the north of the ice shelf and one site in the south. The profiles show that the water column at the sites are composed of ISW, and the θ-S characteristics show no evidence of water above the surface freezing point entering the cavity. The currents in the south are dominated by tides, with a weak mean flow from east to west. Temperature and current data from the boundary layer at the southern site suggest a mean melt rate of around 1.9 m a^{-1} for the 8-day duration of the available record, compared with a radar-derived value of 1.3 ± 0.2 m a^{-1} over the same period.

[27] The evidence suggests that the salinity of the water that enters the cavity is between 34.60 and 34.65. The upper limit suggests that the inflowing water is not HSSW formed originally over the Ronne continental shelf, but is a result of wintertime cooling and salinification of MWDW that has crossed the shelf break locally. The low temperature (−1.96°C) of the westward-flowing water at the southern site suggests that the inflowing HSSW has interacted with thin ice to the south of Kenyon Peninsula before entering the main cavity.

[28] We conclude that there is no evidence of water above the surface freezing point in the sub-Larsen C Ice Shelf cavity, and that the ice shelf's basal melt rate has not been increasing significantly during the period for which oceanographic data are available.

[29] Our analysis is based on snapshots from different years, and none of these are from the winter (although observed conditions at the northern site are arguably responding to winter conditions at the ice front). It is possible that large interannual variations are confounding the analysis, with the cavity flickering between warm and cold conditions. Multi-year time series are required to resolve this question.

[30] **Acknowledgments.** The authors are grateful to Mike Schröder and one anonymous reviewer, whose comments significantly improved the paper. We are indebted to Paul Anker, Mike Brian, and James Smith and for their support in the field.

[31] The Editor thanks Michael Schröder and an anonymous reviewer for assisting in the evaluation of this paper.

References

Absy, J. M., M. Schröder, R. Meunch, and H. H. Hellmer (2008), Early summer thermohaline characteristics and mixing in the western Weddell Sea, *Deep Sea Res., Part II*, *55*, 1117–1131, doi:10.1016/j.dsr2.2007.12.023.

Bathmann, U., V. Smetacek, H. de Baar, E. Fahrbach, and G. Krause (1994), The expeditions ANTARKTIS X/6-8 of the research vessel "POLARSTERN" in 1992/93, report, 236 pp., Alfred-Wegener Inst., Bremerhaven, Germany.

Book, J. W., P. J. Martin, I. Janeković, M. Kuzmić, and M. Wimbush (2009), Vertical structure of bottom Ekman tidal flows: Observations, theory, and modeling from the northern Adriatic, *J. Geophys. Res.*, *114*, C01S06, doi:10.1029/2008JC004736.

Cochran, J. R., and R. E. Bell (2012), Inversion of IceBridge gravity data for continental shelf bathymetry beneath the Larsen Ice Shelf, Antarctica, *J. Glaciol.*, *58*(209), 540–552, doi:10.3189/2012JoG11J033.

Foldvik, A., T. Gammelsrød, N. Slotsvik, and T. Tørresen (1985), Oceanographic conditions on the Weddell Sea Shelf during the German Antarctic Expedition 1979/80, *Polar Res.*, *3*(2), 209–226, doi:10.1111/j.1751-8369.1985.tb00508.x.

Gade, H. G. (1979), Melting of ice in sea water: A primitive model with application to the Antarctic ice shelf and icebergs, *J. Phys. Oceanogr.*, *9*(1), 189–198, doi:10.1175/1520-0485(1979)009<0189:MOIISW>2.0.CO;2.

Gordon, A. L. (1998), Western Weddell Sea thermohaline stratification, in *Ocean, Ice and Atmosphere: Interactions at the Antarctic Continental Margin*, *Antarct. Res. Ser.*, vol. 75, edited by S. S. Jacobs and R. F. Weiss, pp. 215–240, AGU, Washington, D. C., doi:10.1029/AR075p0215.

Grosfeld, K., R. Gerdes, and J. Determann (1997), Thermohaline circulation and interaction between ice shelf cavities and the adjacent open ocean, *J. Geophys. Res.*, *102*, 15,595–15,610, doi:10.1029/97JC00891.

Hellmer, H. H., M. Schröder, C. Haas, G. S. Dieckmann, and M. Spindler (2008), The ISPOL drift experiment, *Deep Sea Res., Part II*, *55*, 913–917, doi:10.1016/j.dsr2.2008.01.001.

Hellmer, H. H., O. Huhn, D. Gomis, and R. Timmermann (2011), On the freshening of the northwestern Weddell Sea continental shelf, *Ocean Sci.*, *7*, 305–316, doi:10.5194/os-7-305-2011.

Holland, P. R., F. J. C. Corr, D. G. Vaughan, A. Jenkins, and P. Skvarca (2009), Marine ice in Larsen Ice Shelf, *Geophys. Res. Lett.*, *36*, L11604, doi:10.1029/2009GL038162.

Holland, P. R., H. F. J. Corr, H. D. Pritchard, D. G. Vaughan, R. J. Arthern, A. Jenkins, and M. Tedesco (2011), The air content of Larsen Ice Shelf, *Geophys. Res. Lett.*, *38*, L10503, doi:10.1029/2011GL047245.

Jenkins, A., K. W. Nicholls, and H. F. J. Corr (2010), Observation and parameterisation of ablation at the base of Ronne Ice Shelf, Antarctica, *J. Phys. Oceanogr.*, *40*, 2298–2312, doi:10.1175/2010JPO4317.1.

Lythe, M. B., and D. G. Vaughan (2001), BEDMAP: A new ice thickness and subglacial topographic model of Antarctica, *J. Geophys. Res.*, *106*, 11,335–11,351, doi:10.1029/2000JB900449.

Munk, W. H., and D. E. Cartwright (1966), Tidal spectroscopy and prediction, *Philos. Trans. R. Soc. London, Ser. A*, *259*, 533–581, doi:10.1098/rsta.1966.0024.

Nicholls, K. W., C. J. Pudsey, and P. Morris (2004), Summer time water masses off the northern Larsen C Ice Shelf, Antarctica, *Geophys. Res. Lett.*, *31*, L09309, doi:10.1029/2004GL019924.

Pritchard, H. D., S. R. M. Ligtenberg, H. A. Fricker, D. G. Vaughan, M. R. van den Broeke, and L. Padman (2012), Antarctic ice-sheet loss driven by basal melting of ice shelves, *Nature*, *484*, 502–505, doi:10.1038/nature10968.

Rignot, E., J. Mouginot, and B. Scheuchl (2011), Ice flow of the Antarctic Ice Sheet, *Science*, *333*, 1427–1430, doi:10.1126/science.1208336.

Shepherd, A., D. J. Wingham, T. Payne, and P. Skvarca (2003), Larsen Ice Shelf has progressively thinned, *Science*, *302*, 856–859, doi:10.1126/science.1089768.

Vautard, R., P. Yiou, and M. Ghil (1992), Singular-spectrum analysis—A toolkit for short, noisy chaotic signals, *Physica D*, *58*, 95–126, doi:10.1016/0167-2789(92)90103-T.